ACS OMEGA

Open Access

http://pubs.acs.org/journal/acsodf

Article

Simulation and Experimental Study of Solid−Liquid Extraction of Coal Tar Residue Based on Different Extractants

Bo Yang, Xiaoyong Fan,* Dong Li, Louwei Cui, Chunran Chang, Long Yan, Bowang Lu, and Jian Li

Cite This: *ACS Omega* 2023, 8, 47835−47845

Read Online

ACCESS | Metrics & More | Article Recommendations

ABSTRACT: Coal tar residue (CTR) is recognized as a hazardous industrial waste with a high carbon content and coal tar consisting mainly of toxic polycyclic aromatic hydrocarbons (PAHs). The coal tar in CTR can be deeply processed into high-value-added fuels and chemicals. Effective separation of coal tar and residue in CTR is a high-value-added utilization method for it. In this paper, ethyl acetate, ethanol, and *n*-hexane were chosen as extractants to study the extraction process of coal tar from CTR, considering the mass transfer in the liquid phase outside the CTR particles and the diffusion inside the CTR particles, and a mathematical model of the solid−liquid extraction process of CTR was established based on Fick's second law. First, the mass-transfer coefficients (k_f) and effective diffusion coefficients (D_e) of ethyl acetate, ethanol, and *n*-hexane in solid−liquid extraction at 35 °C were determined to be 1.54×10^{-5} and 4.99×10^{-10} $m^2 \cdot s^{-1}$, 1.14×10^{-5} and 3.57×10^{-10} $m^2 \cdot s^{-1}$, and 1.01×10^{-5} and 3.48×10^{-10} $m^2 \cdot s^{-1}$, respectively. Furthermore, the simulated values obtained by the model also maintained a high degree of agreement with the experimental results, which indicates the high accuracy prediction of the model. Finally, the model was used to investigate the effects of the solvent−solid ratio, temperature, and stirring speed on the extraction rates with the three extractants. According to the analysis with gas chromatography−mass spectrometry (GC-MS), among the three solvents, *n*-hexane extracted the highest content of aliphatic hydrocarbons (ALHs), ethyl acetate extracted the highest content of oxygenated compounds (OCs), and ethanol extracted the highest content of aromatic hydrocarbons (ARHs). The model and experimental data can be used to provide accurate predictions for industrial utilization of CTR.

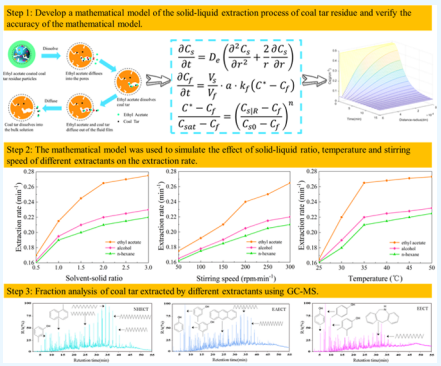

1. INTRODUCTION

During the coal pyrolysis process, high-boiling-point organic compounds condense to form coal tar. At the same time, coal dust, coke dust, and ash entrained in the gas are mixed into the coal tar and form agglomerates of different sizes called CTR.[1,2] CTR can be divided into coking CTR, medium- and low-temperature pyrolysis CTR, and fixed bed gasification CTR based on the different processing technologies. CTR is a porous structured substance with a porosity of 63−68%, low ash content of 4−8%, high fixed carbon of 55−60%, and volatile substances of 33−37%.[3]

Currently used methods for CTR, as reported, included blending with coal, using as a fuel, converting into fuel oil, and producing activated carbon.[3,4] The CTR contains large amounts of 2−6 ring aromatic hydrocarbons, some of which are carcinogenic PAHs, such as naphthalene and benzo[*a*]-pyrene, and their direct emissions can cause serious contamination of soil, water, and air.[5−7] PAHs are mainly distributed in coal tar, so separating coal tar from CTR can reduce its environmental hazards.[8]

The CTR solid−liquid extraction is a widely used technology for separating coal tar from the CTR solid matrix, which have the characteristics of easy operation and high efficiency.[9−11] The process of dissolving coal tar in CTR begins with the solvent reaching the solid phase so that coal tar can be extracted deeper into the solid structure of the CTR. The solvent needs to penetrate through the pores to dissolve the coal tar in the dense CTR matrix. Because of the concentration difference between the coal tar in the matrix and the coal tar in the solvent main solution, the coal tar dissolved into the solvent will diffuse to the surface of the CTR particles from the inside through the pores. Finally, the coal tar then reaches the solvent main solution from its surface through the fluid membrane. The solid−liquid extraction process can be divided into three consecutive stages: immersion, dissolution, and diffusion, as shown in Figure 1.[12]

The following 5 steps may be distinguished in the process:

(1) Solvent immersion of solid (particle) surfaces.

(2) Diffusion and penetration of the solvent into the internal micropores of the solid (particles).

Received: August 24, 2023
Revised: October 22, 2023
Accepted: November 22, 2023
Published: December 6, 2023

https://doi.org/10.1021/acsomega.3c06290
ACS Omega 2023, 8, 47835−47845

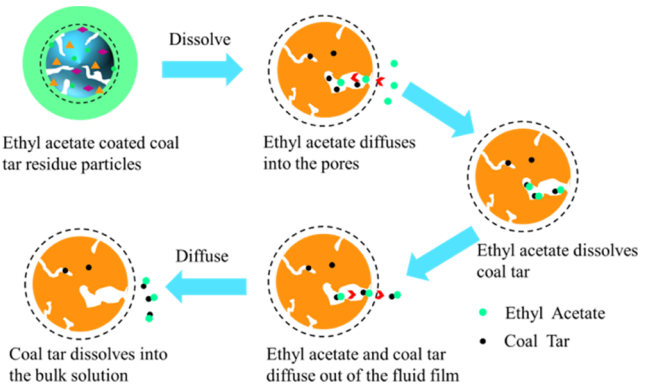

Figure 1. Process of extracting coal tar with ethyl acetate.

(3) Desorption of the solute into the solvent.
(4) Internal diffusion of solutes to the surface of solids (particles).
(5) The solute diffuses from the solid surface to the solvent body across the fluid film.

Ho et al.[13] used a diffusion model and a two-site kinetic model to describe the extraction of lignin from flaxseed meal by pressurized low-polarity water, and the fitted curves of both models were in high accordance with the experimental data. Sánchez et al.[14] established a kinetic model for the diffusion of polyphenols in grape pomace by water and ethanol extraction based on Fick's second law, and the correlation coefficients R^2 > 0.989 for this model were obtained from the experimental data and were in good accordance with the experimental data. Wang et al.[15] established a solid–liquid extraction diffusion kinetic model for lignite wax based on experimental and theoretical analysis, which not only predicted the extraction yield of lignite wax in the Greif extractor but also estimated the concentration in a specific region during the extraction process. Wongkittipong et al.[16] researched the kinetic response of solid–liquid extraction of ethanol–water solvent from the leaves and stems of *Andrographis paniculata* and proposed a kinetic model for solid–liquid extraction, which had a correlation coefficient R^2 = 0.9978 and remained in high agreement with the experimental results.

Simeonov et al.[17] solved the model of a tribulus–ethanol solid–liquid system in a stirred vessel using a specific function. Sánchez et al.[14] calculated k_f for the extraction of polyphenols from white grape pomace in a stirred vessel using the correlation of spherical particle beds proposed by Perry and Green,[18] and the research has shown that the critical parameters impacting the dynamics of solid–liquid extraction are D_e and k_f.[19−22] The k_f controls the external fluid film resistance, which is determined by the hydrodynamic conditions and the fluid properties of the solvent. The pore geometry, porosity, and connectivity of porous media are parameters that affect D_e, which is specific in each porous media.

As mentioned above, researchers have studied the solid–liquid extraction process of different systems by establishing kinetic models, but there is a lack of specialized research on CTR systems. Therefore, this research can provide valuable insights into the extraction of CTR systems. In the CTR solid–liquid extraction process, k_f and D_e values were calculated for three different extractants. The accuracy of the mathematical model was verified through experimental data and theoretical calculations. The mathematical model was then utilized to examine the impact of the solvent–solid ratio, temperature, and stirring speed on the extraction rates of the three extractants.

2. EXPERIMENTAL SECTION

2.1. Experimental Materials and Methods. In this paper, the raw material CTR was collected from Yulin Shenmu Fu Oil Energy Technology Company, and ethyl acetate, ethanol, and *n*-hexane, AR grade, with purity ≥99% were selected as extraction solvents and obtained from Tianjin Comio Chemical Reagent Co. The experiments were carried out by thermal extraction–decompression filtration in a 100 mL stirred reactor, as shown in Figure 2.

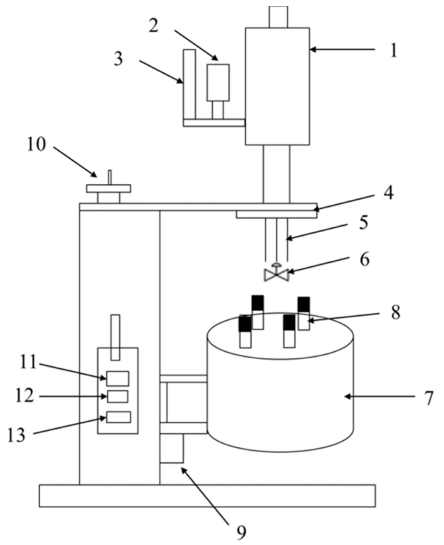

Figure 2. Extraction device ((1) magnetically coupled stirring, (2) pressure gauge, (3) pressure sensor, (4) kettle lid, (5) sampling probe bottom tube, (6) impeller, (7) heating furnace, (8) high-pressure bolt, (9) lifting mechanism, (10) hand wheel, (11) Ethernet port, (12) RS485 port, and (13) power switch).

The CTR and the extractant were added into the stirred reactor according to a certain mass–volume ratio and heated to 30–50 °C with constant stirring for 15 min. After the extraction was completed, the liquid-phase filtrate and solid-phase filter cake were obtained by filtration under reduced pressure. The filter cake was dried in a vacuum drying oven and weighed after drying was completed. The filtrate was distilled under reduced pressure to separate the extractant from the coal tar, and the extractant was recycled; the complete experimental flow is shown in Figure 3.

2.2. Characterization and Analysis of CTR. The surface morphology of extraction residue was examined using a ZEISS Sigma 300 field-scanning electron microscope (SEM) at an accelerating voltage of 10 kV. As illustrated in Figure 4, CTR exhibits agglomerated structures along with dense particles, encompassing a broad size range of 20–300 μm. Notably, the substantial presence of micropores on the surface of CTR indicates its porous structure as a solid industrial waste. Therefore, it may be inferred that part of the tar is probably adsorbed inside the micropores.[23] This porous structure indicates the possible occurrence of pore diffusion during the solid–liquid extraction process of CTR and can support the assumption of CTR as a porous spherical model in this paper.

https://doi.org/10.1021/acsomega.3c06290
ACS Omega 2023, 8, 47835−47845

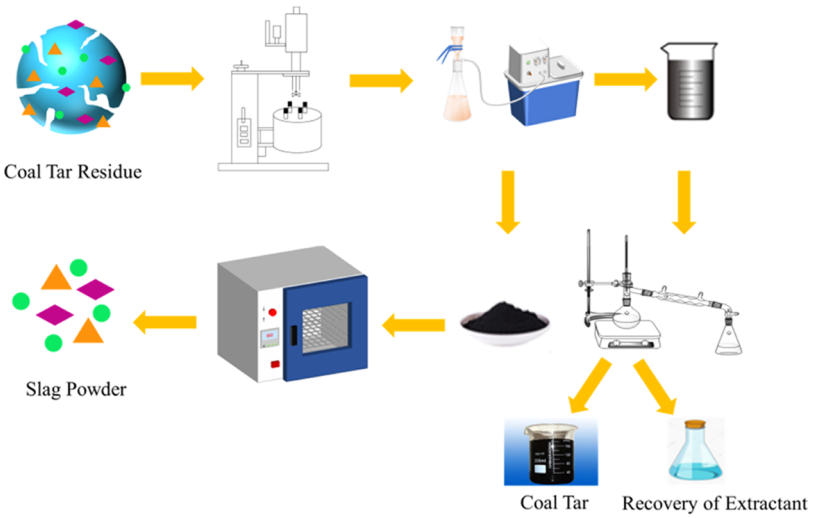

Figure 3. Experimental flow.

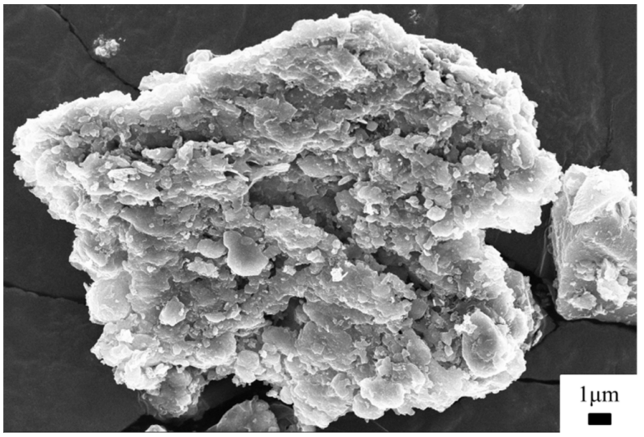

Figure 4. SEM analysis of the extraction residue.

The particle size analysis of the extraction residue was performed by using a Malvern Mastersizer 3000 laser particle size meter. As illustrated in Figure 5, particles with sizes below 19.1 μm constitute approximately 10% of the total extraction residue volume, while those in the range of 19.1−44.7 μm account for approximately 15%. Moreover, particles in the range of 44.7−96.1 μm represent about 25%, followed by particles in the range of 96.1−182 μm, which contribute approximately 25%. Additionally, particles within the range of 182−298 μm comprise around 15% of the total volume, while particles larger than 298 μm constitute approximately 10% of the overall volume. It is revealed that the skeletal particles forming the CTR account for roughly 54% of the whole below 100 μm, and the particle size distribution ranges from 1 to 660 μm, with a volume-average particle size of 132 μm. The particle size analysis data can provide information for the mathematical model established. The volume-averaged particle size of CTR was calculated by eq 1

$$D[4, 3] = \sum_{i=1} f_i \times D_i \tag{1}$$

where D_i denotes the average particle size of the i-th size interval and f_i denotes the percentage of the i-th size interval.

2.3. Analytical Method for the Organic Composition of Extracted Coal Tar. In this paper, an Agilent 8890/5977B GC-MS instrument was used, and the specific parameters were set. An Agilent HP-5MS column was used with a film thickness of 0.25 μm, an inner diameter of 250 μm, a column length of 60 m, and a carrier gas of helium. The initial temperature of the GC chamber was set at 60 °C, the flow rate was 1.2 mL·min^{-1}, the temperature increase rate was 5 or 10°C·min^{-1}, the final temperature was 300 °C, and the retention time was 10 min. The MS was performed with an electron bombardment ion source (EI) as the ion source, with a shunt ratio of 20:1,

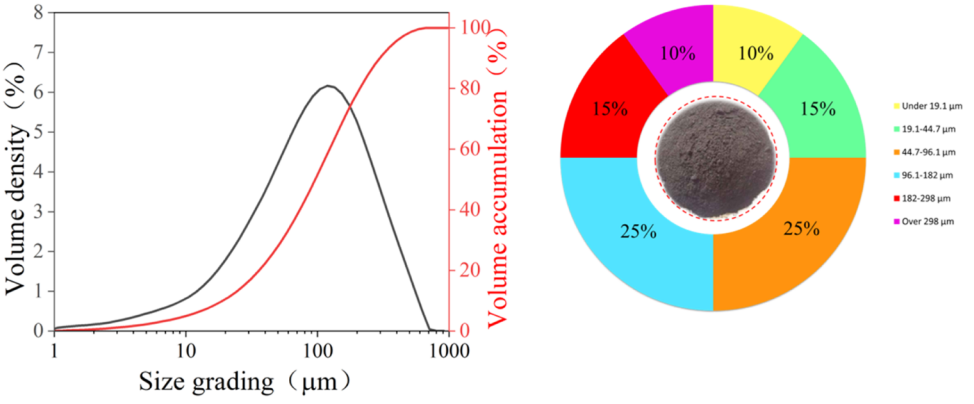

Figure 5. Particle size analysis and particle size distribution of extraction residue.

https://doi.org/10.1021/acsomega.3c06290
ACS Omega 2023, 8, 47835−47845

bombardment voltage of 70 eV, and m/z acquisition range of 33−550.

3. ESTABLISHING A MATHEMATICAL MODEL FOR SOLID−LIQUID EXTRACTION

The CTR solid−liquid extraction process is complex, and the establishment of mathematical models can help to understand the extraction process mechanism and provide an accurate prediction of the extraction rate of different extractants at different process parameters.

In this paper, the model was first simplified on the basis of reasonable assumptions to establish a mathematical model of solid−liquid extraction based on Fick's second law. Next, the model parameters are obtained by calculating k_f and D_e according to the empirical formula. The model was then solved using the ODE solver of MATLAB software to obtain the simulated values of CTR solid−liquid extraction and compared with the experimental values to verify the accuracy of the model.[24] Finally, the effects of the solvent−solid ratio, temperature, and stirring speed on the CTR extraction rate were investigated based on the model.

3.1. Model Assumptions. This experiment was done in a 100 mL stirred reactor with a small equipment size and a constant heating temperature; therefore, it is considered an isothermal system in the stirred reactor. Appropriate simplification of the model is extremely important for the establishment of the mathematical model, both to ensure the association of key factors that have a large impact on the overall reaction system and to remove the less influential unfavorable factors, and to simplify the computational conditions of the model within a reasonable range to achieve rapid convergence in the solution process.[25] The particles in the CTR are pulverized coal and coke powder from coal pyrolysis; thus, the following assumptions are made to simplify the model

(1) CTR particles are spherical homogeneous granules with micropores, the particles are covered with an external fluid film, and the particle size is evenly distributed, as shown in Figure 6.

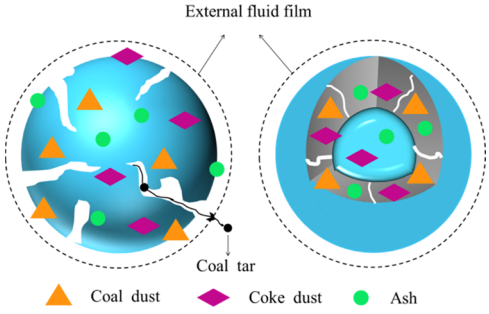

Figure 6. Particle model of CTR.

(2) The extraction process is a steady-state isothermal operation.
(3) The effective diffusion coefficient of the solvent inside the particle is constant.
(4) The presence of only one type of solute in the material, i.e., a pseudocomponent.
(5) Disregarding the vaporization of the oil and solvent phases, the volumes of both do not change throughout the process.
(6) The physical properties of the solvent and CTR were constant during the extraction process.

3.2. Mathematical Model of the Stirred Reactor. Usually, the rate of solid−liquid extraction depends on the diffusion phase and the concentration difference between the inside and outside of the solid particles. The driving force of diffusion is influenced by the particle structure, the nature of the solvent, and the flow field (the effect of the temperature is not considered here for the time being). The mass balance of solid particles and the solvent is the most important conservation equation describing the solid−liquid extraction mechanism, and the general conservation equation for the nonsteady diffusion of solutes inside spherical particles when their concentration diffusion varies with time is known as Fick's second law.[26,27] According to this law, the mass balance equation for solid particles can be written as eq 2

$$\frac{\partial C_s}{\partial t} = D_e\left(\frac{\partial^2 C_s}{\partial r^2} + \frac{2}{r}\frac{\partial C_s}{\partial r}\right) \tag{2}$$

$$\text{initial conditions: } t = 0,\ C_s = C_{s0} \tag{3}$$

$$\text{boundary conditions: } r = 0,\ \frac{\partial C_s}{\partial r} = 0 \tag{4}$$

$$r = R,\ D_e\left(\frac{\partial C_{s|R}}{\partial r}\right) = -k_f(C^* - C_f) \tag{5}$$

The differential mass balance equation for the solute can be written as

$$\frac{\partial C_f}{\partial t} = -\frac{V_s}{V_f}\frac{\partial \overline{C_s}}{\partial t} = \frac{V_s}{V_f}\cdot a\cdot k_f(C^* - C_f) = \frac{a\cdot k_f(C^* - C_f)}{R_b} \tag{6}$$

where $R_b = V_f/V_s$ is defined as the ratio of the solvent volume to the solid-phase volume; $V_s = V\cdot B$ is the volume of the solid phase; $V_f = V(1 - B)$ is the volume of the liquid phase in the extractor; $V = \pi R_c^2 L$ is the volume of the extractor; R_c is the radius of the extractor;$B = \frac{V_s}{V_f + V_s(1-\varepsilon_p)}$ is the volume ratio of the extractor, which is the ratio of the volume of the raw material to the total volume;$\overline{C_s}$ is the average concentration of solute in the solid particles; and $a = \frac{4\pi R^2}{4/3\pi R^3} = \frac{3}{R}$ is the specific surface area of the particles.

The Freundlich isotherm is widely used in nonlinear equilibria.[26] This model applies to a specific equilibrium relationship between the concentration of solute at the surface of the particle and the concentration of solute inside the particle at the infinitesimal $r = R$. The extraction equilibrium relationship can be written as[28]

$$\frac{C^* - C_f}{C_{sat} - C_f} = \left(\frac{C_{s|R} - C_f}{C_{s0} - C_f}\right)^n \tag{7}$$

where parameter $n \approx 2$.[12] The relationship between the magnitudes of the concentrations in equation is $C_f < C^* \le C_{sat}$ and $C_f < C_s \le C_{s0}$.

3.3. Solution of the Model Parameters. k_f and D_e are two extremely important parameters in the study of extraction processes. k_f indicates the amount of material transferred from one phase into another phase per unit concentration, per unit

https://doi.org/10.1021/acsomega.3c06290
ACS Omega 2023, 8, 47835−47845

area, per unit time, and can reflect the degree of intensification of a specific mass-transfer process. D_e indicates the ability of a solvent to diffuse in a porous solid and is a physical property of the substance. The basic parameters of the different extractants are shown in Table 1. The basic parameters of the CTR and stirred reactor are shown in Table 2.

Table 1. Basic Parameters of Different Extractants

parameter	ethyl acetate	ethyl alcohol	*n*-hexane
viscosity μ_B (mPa·s)	0.48	0.594	0.68
association factor of solvent φ	1	1.5	1
the density of the liquid ρ (g·cm^{-3})	0.902	0.7893	0.659
the molecular mass of solvent M_B (g·mol^{-1})	88.105	46.07	86.175

Table 2. Basic Parameters of Coal Tar Residue and Stirring Reactor

parameter	numerical value
time (min)	15
solvent volume (mL)	60
coal tar residue weight (g)	20
liquid−solid ratio R_b (−)	3
mean particle size (mm)	0.132
length of stirred reactor (cm)	10
extraction temperature (K)	308.15
stirring speed (rpm·min^{-1})	300
the radius of the reactor (cm)	5
the density of the liquid ρ (g·cm^{-3})	0.902
the porosity of the solid particle ε_p (−)	0.63
the specific surface area of the particle (m^2·g^{-1})	0.44
the initial concentration of coal tar C_{s0} (g·cm^{-3})	0.48
the concentration of saturated solute C_{sat} (g·cm^{-3})	0.30
molar volume of ethyl acetate at boiling point V_A (cm^3·moL^{-1})	489

3.3.1. Solution of the Mass-Transfer Coefficient k_f. The factors influencing k_f are the fluid density, fluid viscosity, binary diffusion coefficient, qualitative size, and fluid speed. Based on the influencing factors of k_f, the function of k_f is written as eq 8

$$k_f = f(\rho, \mu, u, D_T, D_{AB}) \tag{8}$$

where D_{AB} represents the binary diffusion coefficient of solute A in solvent B, estimated from the Wilke−Chang equation. Equation 9 is used to describe the two-dimensional diffusivity

$$D_{AB} = 7.4 \times 10^{-8}(\varphi \cdot M_B)^{0.5} \frac{T}{\mu_B \cdot V_A^{0.6}} \tag{9}$$

where M_B is the molecular weight of substance B, V_A is the molar volume of solute A at the boiling point in the normal state (cm^3·moL^{-1}), μ_B is the viscosity of substance B (mPa·s), T is the temperature (K), and φ is the association factor of solvent B.

k_f can be obtained by establishing a relationship between the Sherwood number (Sh) and the binary diffusion coefficient D_{AB}, as shown in eq 10

$$\mathrm{Sh} = k_f D_T / D_{AB} \tag{10}$$

Schmidt number (Sc) represents the ratio of kinematic viscosity coefficient and diffusion coefficient and describes fluids with both momentum and mass diffusion. Sc was calculated using the Stokes−Einstein empirical equation,[29] as described in eq 11

$$\mathrm{Sc} = \mu / \rho D_{AB} \tag{11}$$

Reynolds number is a dimensionless number that can be used to characterize the flow of a fluid. The Reynolds number (Re_T) in the mixing vessel is related to the flow speed, density, viscosity coefficient, and characteristic length of the fluid, as shown in eq 12

$$\mathrm{Re}_T = \rho u D_T / \mu \tag{12}$$

Combining eqs 8−12, the function of the Sherwood number can be obtained, as presented in eq 13

$$\mathrm{Sh} = f(\mathrm{Re}_T, \mathrm{Sc}) \tag{13}$$

Sherwood number is the ratio of convective mass transfer to diffusive mass transfer. Humphrey and Ness[30] determined the mass-transfer coefficient of dissolved $Na_2S_2O_3{\cdot}5H_2O$ and proposed a relation to calculate the particle-liquid mass-transfer coefficient in a stirred vessel under steady flow conditions by comparing it with previous results, as shown in eq 14

$$\mathrm{Sh} = 0.0032(\mathrm{Re}_T)^{0.87}\mathrm{Sc}^{0.5} \tag{14}$$

According to eqs 8−14 and the data in Tables 1 and 2, the D_{AB} and k_f of different extractants in the extraction process can be obtained after calculation, as shown in Table 3.

Table 3. Calculated D_{AB} and k_f Values of Different Solvents

solvent	D_{AB} (m^2·s^{-1})	k_f (m·s^{-1})
ethyl acetate	10.85×10^{-10}	1.54×10^{-5}
ethanol	7.77×10^{-10}	1.14×10^{-5}
n-hexane	7.58×10^{-10}	1.01×10^{-5}

3.3.2. Solution of the Effective Diffusion Coefficient D_e. D_e is mainly used for the diffusion of fluids in porous solids. The zigzag factor and diffusion coefficient were expressed by Wakao and Smith[31] as a power of the particle porosity ε_p and $D_e = D_{AB}\varepsilon_p^n$, respectively. In addition to Chang[32] who expressed the curvature factor $2 - \varepsilon_p$, Goto et al.[20] and Ndocko et al.[21] applied $D_e = D_{AB}{\cdot}\varepsilon_p/(2 - \varepsilon_p)$ to estimate D_e for lignin extracted from white fir sapwood and natural active compounds extracted from plants. Based on previous studies and CTR properties, eq 15 will be chosen as the effective diffusion coefficient relationship equation for CTR in solid−liquid extraction in this study.

$$D_e = D_{AB}{\cdot}\varepsilon_p/(2 - \varepsilon_p) \tag{15}$$

The specific values of D_e for different extractants obtained according to eq 14 are shown in Table 4.

3.3.3. Solution of the Mathematical Model. In this paper, the ODE solver of MATLAB software is used to solve the differential mass balance in eq 2 for solid particles based on the system of PDE equations of PDEPE functions. The ODE solver may offer a matrix to set up each differential equation

Table 4. Calculated Values of D_e for Different Solvents

parameter	ethyl acetate	ethanol	*n*-hexane
D_e(m^2·s^{-1})	4.99×10^{-10}	3.57×10^{-10}	3.48×10^{-10}

https://doi.org/10.1021/acsomega.3c06290
ACS Omega 2023, 8, 47835−47845

and boundary condition, and the time for a single computation of the numerical solution relies on the time step, which is changed using the self-tuning algorithm in the MATLAB solver ODE15s.[33] Equation 2 is transformed into the PDE equation format according to the PDEPE function as shown in eq 16

$$c\left(x, t, u, \frac{\partial u}{\partial x}\right)\frac{\partial u}{\partial t} = x^{-m}\frac{\partial}{\partial x}\left(x^{m} f\left(x, t, u, \frac{\partial u}{\partial x}\right)\right) + s\left(x, t, u, \frac{\partial u}{\partial x}\right) \tag{16}$$

In this form, the PDE coefficients are matrix values and the equation becomes

$$\begin{bmatrix}1\\1\end{bmatrix}\begin{bmatrix}\frac{\partial C_s}{\partial t}\\ \frac{\partial C_f}{\partial t}\end{bmatrix} = \frac{\partial}{\partial r}\begin{bmatrix}D_e\frac{\partial C_s}{\partial r}\\ 0\cdot\frac{\partial C_f}{\partial r}\end{bmatrix} + \begin{bmatrix}2D_e\frac{\partial C_s}{\partial r}\\ C_{sat}\left(\frac{C_s}{C_{s0}}\right)^2\cdot C_f\end{bmatrix} \tag{17}$$

Boundary conditions

$$r = 0, \frac{\partial C_{si}}{\partial r} = 0 \tag{18}$$

$$r = 0, D_e\frac{\partial C_{si}}{\partial r} = -k_f(C^* - C_{fi}), C^* = f(C_{si,n}) \tag{19}$$

where C_{si} is the concentration of the solute at the time t_i and C_{fi} is the concentration of the solute in the solvent at the time t_i.

In this article, ethyl acetate was chosen as the solvent for CTR extraction. According to the above solution process, the variation of coal tar concentration during the extraction of CTR particles by ethyl acetate in the stirred reactor can be obtained, and Figure 7 gives the trend of coal tar concentration

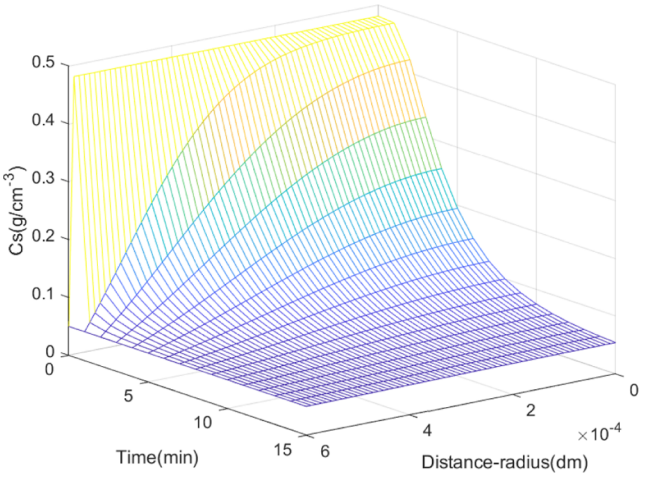

Figure 7. Variation of the coal tar concentration with time and location during ethyl acetate extraction by CTR particles.

of CTR particles during solid−liquid extraction with the extraction time and the position of particle radius r. In the solution, the CTR particle radius was divided into 60 regions with a time discretization of 1 min and an extraction time of 15 min.

According to Figure 7, the concentration of coal tar inside the particles showed a gradient distribution after the extraction started; the concentration of coal tar at the center of the particles was the highest; and the concentration of coal tar at the outermost end of the particles was the lowest. The coal tar concentration gradient almost no longer changes after t = 15 min, which indicates that the coal tar concentration inside the particles has reached equilibrium.[34,35] It was also found that the coal tar was extracted more quickly closer to the outer end of the particles, while the coal tar closer to the center of the particles was difficult to be extracted. This may be attributed to the short diffusion distance of coal tar near the outer end of the particle, the long diffusion distance of coal tar in the central part of the particle, and the complex internal structure of the pore space which is also an obstacle in the diffusion process.[36]

4. RESULTS AND DISCUSSION

4.1. Validation of the Model. In this article, the accuracy of the above mathematical model was verified by the experimental data of CTR extraction with ethyl acetate. The numerical solution of the CTR extraction rate in the stirred reactor was calculated by eq 20

$$Y_{sim}(t_i) = (C_{s0} - \overline{C}_s)/C_{s0} \tag{20}$$

The average solute concentration of CTR particles is calculated as shown in eq 21

$$\overline{C}_s = \frac{1}{V_p}\int_0^R 4\pi r^2 C_s(r)\mathrm{d}r \tag{21}$$

where V_p is the volume of each CTR particle, $V_p = 4/3\pi R^3$. In this paper, the trapezoidal composite formula (eq 22) is used to calculate the integral in eq 21 and the converted estimated $\overline{C}_s$. The trapezoidal formula is shown in eq 23

$$\int_0^L f(z)\mathrm{d}z \approx \frac{\Delta z}{2}\left(f(0) + 2\sum_{j=1}^{n-1} f(z_j) + f(L)\right) \tag{22}$$

$$\overline{C}_s(i) \approx \frac{1}{V_p}\cdot\frac{\Delta z}{2}\cdot\left(f(r_0) + 2\sum_{k=1}^{n-1} f(r_k) + f(r_n)\right) \tag{23}$$

where $f(r_k) = 4\pi r^2\cdot C_s(i, k)$, $r_k = \frac{R}{n}\cdot k$.

According to the above process using MATLAB software for solving equation, the variation law of the extraction rate with time can be simulated and compared with the experimental data, as shown in Figure 8.

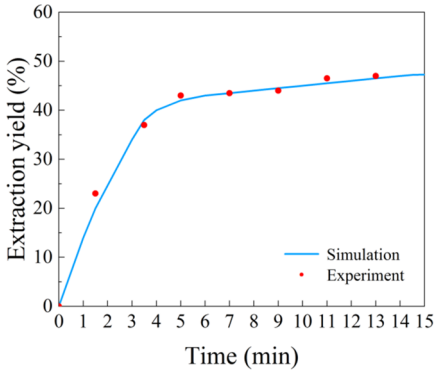

Figure 8. Comparison between simulated and experimental yield.

https://doi.org/10.1021/acsomega.3c06290
ACS Omega 2023, 8, 47835−47845

According to Figure 8, it can be found that the extraction rate of coal tar by ethyl acetate is the fastest in the time of 0−4 min, and the extraction rate has reached more than 35% in the extraction time of 4 min. The extraction rate has increased about 20% in the time of 4−15 min, and the extraction rate enhancement was relatively slow during this period compared to that of 0−4 min.

The best fit between the models was evaluated using standard deviation (SD) and root-mean square (RMS),[37−39] and the mean relative error of model fit ($\overline{E_r}$) was calculated by eq 24, and SD and RMS were calculated by eqs 25 and 26, respectively.

$$\overline{E_r} = \frac{1}{N}\sum_{i=1}^{N}\left|\frac{y_{\mathrm{cal}(i)} - y_{\exp(i)}}{y_{\exp(i)}}\right| \tag{24}$$

$$\mathrm{SD} = \sqrt{\frac{1}{N-1}\sum_{i=1}^{N}\left(\left|\frac{y_{\exp(i)} - y_{\mathrm{cal}(i)}}{y_{\exp(i)}}\right| - \overline{E_r}\right)^2} \tag{25}$$

$$\mathrm{RMS} = \sqrt{\frac{1}{N}\sum_{i=1}^{N}\left(\left|\frac{y_{\exp(i)} - y_{\mathrm{cal}(i)}}{y_{\exp(i)}}\right|\right)^2} \tag{26}$$

where N is the number of experiments; $y_{\mathrm{cal}(i)}$ is the simulation of extraction rate,%; and $y_{\exp(i)}$is the experimental extraction rate,%.

The RMS and SD were calculated to be 0.0486 and 0.0412, respectively, and the closer the RMS and SD values are to 0, the better the fitting results are indicated, which proves that the model is reasonable and reliable and may reflect the process of CTR solid−liquid extraction in stirred vessels more accurately.[40]

4.2. Simulation of the Effect of Process Conditions in Different Solvent Extraction Processes. The effect of CTR extraction is usually related to the process conditions, such as solvent−solid ratio, temperature, and stirring speed. In this section, the effects of process conditions, such as solvent−solid ratio, temperature, and stirring speed, on the CTR extraction process are investigated mainly by the extraction rate.

The equation for calculating the solid−liquid extraction rate of CTR is shown in eq 27

$$r_{\mathrm{ext}}(t_0) = \frac{Y_{\mathrm{sim}}(t_1) - Y_{\mathrm{sim}}(t_0)}{t_1 - t_0} \tag{27}$$

where t_1 is the first period, t_0 is the initial timing time, $Y_{\mathrm{sim}}(t_1)$ is the CTR extraction rate at the time t_1, and $Y_{\mathrm{sim}}(t_0)$ is the CTR extraction rate at the time t_0. As can be seen in Figure 6, ethyl acetate extraction of CTR was the fastest in the range of 0−4 min of extraction time. Therefore, this section mainly investigates the effect of process conditions, such as solvent−solid ratio, temperature, and stirring speed, on the extraction rate during the extraction time from 0 to 4 min.

4.2.1. Effect of Solvent−Solid Ratio on the Extraction Process of Different Solvents. Under the conditions of a constant temperature of 35 °C and stirring speed of 300 rpm·min^{-1}, the effects of different solvent−solid ratios of the three solvents and CTR in the range of 0.5−3 on the extraction rate were studied, k_f was calculated according to eq 7, and the results obtained according to the above mathematical model are displayed in Figure 9.

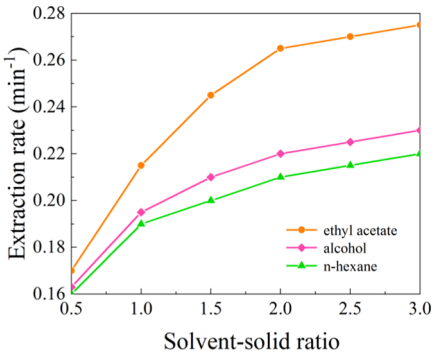

Figure 9. Simulating the effect of solvent−solid ratio on the extraction rate.

The mass of CTR in the stirred reactor was 20 g, and the volume of solvent was 10−60 mL. According to Figure 9, it can be found that the extraction rates of all three solvents were positively correlated with the solvent−solid ratio. The extraction rate was gradually accelerated with the increase of the solvent−solid ratio. The extraction rate of ethyl acetate increased the most in the range of 0.5−2, and the increase gradually began to slow down and tended to the upper boundary when the solvent−solid ratio was greater than 2. The extraction rate of ethanol and *n*-hexane increased the most in the range of 0.5−1 and increased slowly after the ratio was greater than 1. This may be because when the amount of extraction solvent increases, the concentration gradient between the solvent and the coal tar in the CTR increases, resulting in an increase in the mass-transfer rate of coal tar.[34] The upward trend of the extraction rate decreases as the amount of solvent continues to increase. This may be because the higher solvent/solid ratios mean that the ensuing solute separation is more laborious.

4.2.2. Effect of Temperature on the Extraction Process of Different Solvents. Temperature is an important influencing factor in the solid−liquid extraction process. The effects of the three solvents and CTR on the extraction rate at different temperatures in the range 25−50 °C were investigated under the conditions of a constant solvent−solid ratio of 2 and stirring speed of 300 rpm·min^{-1}. Considering the effects of temperature on k_f and D_e, k_f and D_e were corrected for each temperature, and the results obtained from the above mathematical model are shown in Figure 10.

According to Figure 10, it can be found that the extraction rates of all three solvents increase with an increasing temperature. The difference between the extraction rates of

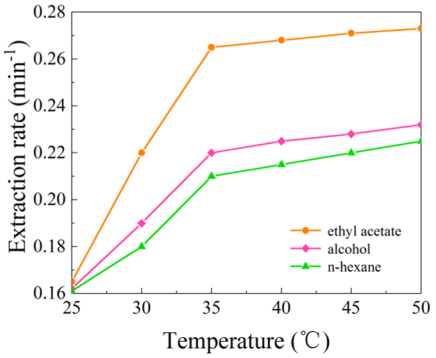

Figure 10. Simulating the effect of temperature on the extraction rate.

https://doi.org/10.1021/acsomega.3c06290
ACS Omega 2023, 8, 47835−47845

the three solvents was small at 25 °C but gradually increased with the increase in temperature. The extraction rate of ethyl acetate was much larger than that of ethanol and *n*-hexane, while the difference between the extraction rates of ethanol and *n*-hexane were small. This may be because with the rise of temperature, the molecular kinetic energy increases; the D_{AB}, D_e, and k_f of coal tar in the three solvents enhances; and the D_{AB}, D_e, and k_f gap of the three solvents also increases. As D_e and k_f increases, the internal and external mass-transfer resistance decreases, thereby increasing the extraction rate.[41]

4.2.3. Effect of Stirring Speed on Different Extraction Processes. The stirring speed is also one of the main factors affecting the solid−liquid extraction process. The effects of the three solvents and CTR on the extraction rate were investigated in the range 50−300 rpm·min^{-1} with different stirring speeds at a solvent−solid ratio of 2 and a temperature of 35 °C. The results calculated according to the above mathematical model are shown in Figure 11.

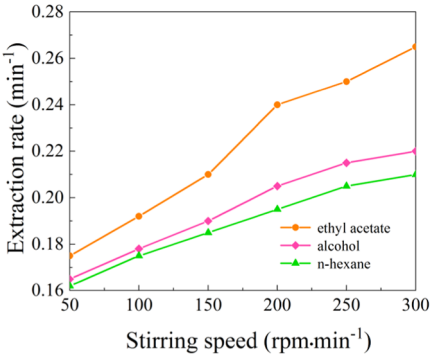

Figure 11. Simulating the effect of stirring speed on the extraction rate.

From Figure 11, it can be found that the extraction rates of the three solvents keep increasing sharply with the increase in the stirring speed. This may be because when the stirring speed increases, the molecular motion is intense, and the CTR particles are mixed more uniformly with the extractant and they are in full contact. When the flow rate of the solution around the surface of the CTR particles is accelerated, the thickness of its surface fluid film decreases.[41] Thus, the mass-transfer resistance from the particle surface to the extractant body becomes smaller, which leads to an increase in the extraction rate.

4.3. GC-MS Analysis of Coal Tar Extracted by Different Solvents. In this paper, an Agilent 7890/5973 GC-MS system was used to analyze the coal tar extracted with different solvents, and it was found that 67 compounds were contained in ethyl acetate-extracted coal tar (EAECT), 70 compounds were contained in *n*-hexane-extracted coal tar (NHECT), and 77 compounds were contained in ethanol-extracted coal tar (EECT), as shown in Figure 12.

Figure 13 reveals the distribution of the components of the different solvent-extracted coal tar such as ALHs, ARHs, OCs, and nitrogen-containing compounds (NCCs). No sulfur-containing compounds (SCCs) were found in the three solvent-extracted coal tar, and NCCs were detected only in the EECT. The percentage of ALH in EAECT was approximately 33.43%, ARH was approximately 34.72%, and OCs was approximately 31.85%. The percentage of ALH in NHECT was approximately 42.48%, ARH was approximately 36.91%, and OCs was approximately 20.61%. The percentage of ALH in EECT was approximately 20.82%, ARH was approximately 38.72%, OCs was approximately 28.79%, and NCCs was approximately 11.67%. Among the three solvents, *n*-hexane extracted the highest content of ALH, ethyl acetate extracted the highest content of OCs, and ethanol extracted the highest content of ARH. This may be because a certain solvent is similar to the solubility parameter and polarity parameter of a certain component, in accordance with the principle of similar dissolution, so that a certain component is high in the extracted coal tar.

4.4. Hydrocarbon Distribution of Coal Tar Extracted with Different Solvents. In this paper, the hydrocarbon fractions of extracted coal tar are categorized into F1, F2, F3, and F4 defined as C_6−C_{10}, C_{10}−C_{16}, C_{16}−C_{34}, and C_{34}−C_{50}, respectively. From Table 5, it can be found that the F1 fraction is 0 in both Zhang et al. and Hu et al. studies, which may be due to evaporation during experimentation or storage.[44] Compared with the sludge recovery oil, no F4 fraction was found in the extracted coal tar. The percentage of the F2 fraction in the extracted coal tar with different solvents was much larger than that in the sludge recovery oil, and on the contrary, the percentage of the F3 fraction in the sludge recovery oil was higher than that of the F3 fraction in the extracted coal tar with different solvents. Only the F2 and F3 fractions were extracted from coal tar by different solvents and differed from each other significantly. In contrast to sludge recovered oil, coal tar was obtained from CTR extraction without the F4 fraction. This is probably due to the absence of F4 fraction in the CTR, which is reported in the literature to be nonexistent in the GC-MS analysis of CTR.[3,43]

5. CONCLUSIONS

In this paper, a simplified mathematical model for solid−liquid extraction of CTR was established based on the experimental data of coal tar extraction from CTR by ethyl acetate in the stirred reactor, considering the mass transfer in the liquid phase outside the CTR particles and the diffusion inside the CTR particles. First, the values of k_f and D_e for the extraction of the three solvents (ethyl acetate, ethanol, and *n*-hexane) were obtained. Second, the established mathematical model was solved numerically using the ODE solver of MATLAB software and verified with the experimental results. Finally, the extraction rates of the three solvents influenced by the factors of solvent−solid ratio, temperature, and stirring speed were investigated. The conclusions are as follows:

(1) The values of k_f and D_e for CTR extraction by ethyl acetate, ethanol, and *n*-hexane at 35 °C were obtained as 1.54×10^{-5} and 4.99×10^{-10} m^2·s^{-1}, 1.14×10^{-5} and 3.57×10^{-10} m^2·s^{-1}, and 1.01×10^{-5} and 3.48×10^{-10} m^2·s^{-1}. k_f and D_e are two parameters that play a decisive role in the solid−liquid extraction process and are positively correlated with the extraction rate. Therefore, the extraction rates of coal tar by the three solvents were in the following order: ethyl acetate > ethanol > *n*-hexane.

(2) A mathematical model of solid−liquid extraction of CTR containing factors such as particle structure, solvent properties, and flow rate field was established, and the model was solved by using MATLAB software to obtain the concentration variation law of coal tar in CTR particles extracted by ethyl acetate. It was found

https://doi.org/10.1021/acsomega.3c06290
ACS Omega 2023, 8, 47835−47845

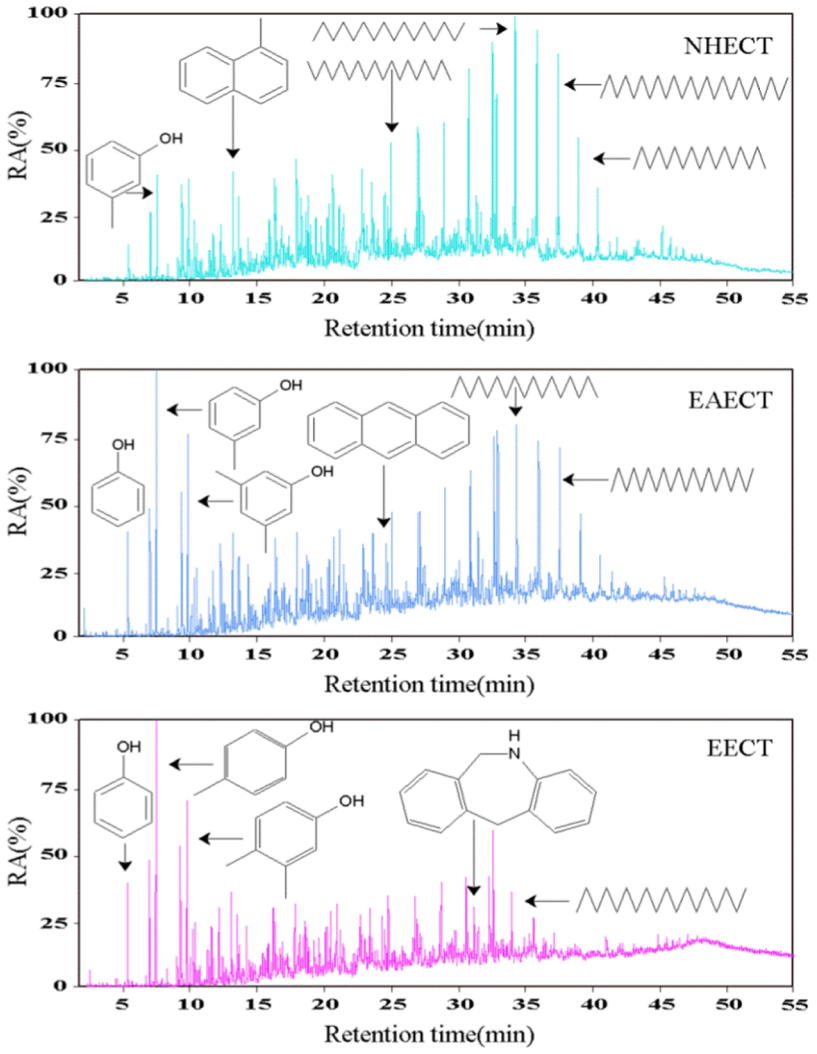

Figure 12. Total ion chromatograms of coal tar extracted from different solvents according to GC-MS analysis.

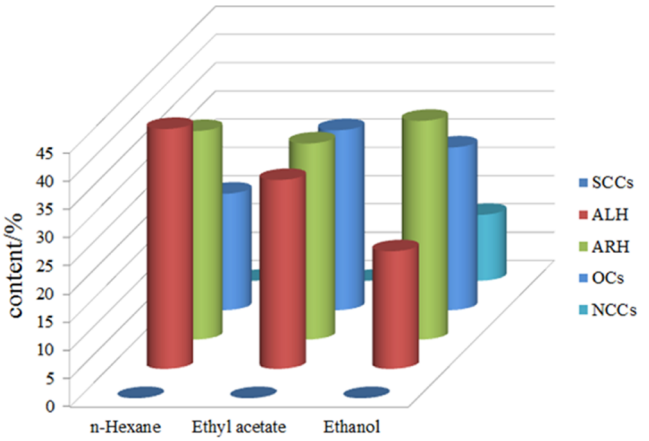

Figure 13. Distribution of components of coal tar extracted from different solvents according to GC-MS analysis.

that the coal tar concentration was the largest at the center of the particles, and the extraction rate was the fastest during 0−4 min and gradually stabilized after 10 min. The RMS of the model was calculated to be 0.0486 and the SD was 0.0412, both close to 0, which demonstrates that the model has an excellent predictive ability.

Table 5. Hydrocarbon Fraction Distribution of Recovered Oil from Sludge and Coal Tar Extracted with Different Solvents

	F1(%)	F2(%)	F3(%)	F4(%)
EAECT	31.85	35.25	32.90	0
NHECT	20.614	36.45	42.936	0
EECT	40.46	35.87	23.67	0
Zhang et al.[44]	0	21.77	64.64	13.37
Hu et al.[42]	0	26.5	69.1	4.3

(3) The effects of solvent−solid ratio, temperature, and stirring speed on the CTR solid−liquid extraction process were researched based on the model. The solvent−solid ratio, temperature, and stirring speed were proportional to the extraction rate for all of the three solvents, and the extraction rate increased gradually with enhance of solvent−solid ratio, temperature, and stirring speed. The trend of increasing extraction rate gradually weakens, which may be due to the gradual saturation of coal tar in the solvents.

(4) Among the three solvents, *n*-hexane has the highest extraction rate for ALH, ethyl acetate has the highest

https://doi.org/10.1021/acsomega.3c06290
ACS Omega 2023, 8, 47835−47845

extraction rate for OCs, and ethanol has the highest extraction rate for ARH. No sulfur-containing compounds (SCCs) were found in the three solvent-extracted coal tar, and NCCs were detected only in the EECT.

AUTHOR INFORMATION

Corresponding Author

Xiaoyong Fan − *School of Chemistry and Chemical Engineering, Shaanxi Key Laboratory of Low Metamorphic Coal Clean Utilization, Yulin University, Yulin 719000, People's Republic of China; School of Chemical Engineering, Northwest University, Xi'an 710069, People's Republic of China;* orcid.org/0000-0002-6351-1778; Phone: +86-15929199059; Email: fanxiaoyong0912@163.com

Authors

Bo Yang − *School of Chemistry and Chemical Engineering, Shaanxi Key Laboratory of Low Metamorphic Coal Clean Utilization, Yulin University, Yulin 719000, People's Republic of China*

Dong Li − *School of Chemical Engineering, Northwest University, Xi'an 710069, People's Republic of China;* orcid.org/0000-0002-4578-0595

Louwei Cui − *The Northwest Research Institute of Chemical Industry, Xi'an 710069, People's Republic of China*

Chunran Chang − *School of Chemistry and Chemical Engineering, Shaanxi Key Laboratory of Low Metamorphic Coal Clean Utilization, Yulin University, Yulin 719000, People's Republic of China; Shaanxi Key Laboratory of Energy Chemical Process Intensification, School of Chemical Engineering and Technology, Xi'an Jiaotong University, Xi'an 710049, People's Republic of China*

Long Yan − *School of Chemistry and Chemical Engineering, Shaanxi Key Laboratory of Low Metamorphic Coal Clean Utilization, Yulin University, Yulin 719000, People's Republic of China*

Bowang Lu − *School of Chemistry and Chemical Engineering, Shaanxi Key Laboratory of Low Metamorphic Coal Clean Utilization, Yulin University, Yulin 719000, People's Republic of China*

Jian Li − *School of Chemistry and Chemical Engineering, Shaanxi Key Laboratory of Low Metamorphic Coal Clean Utilization, Yulin University, Yulin 719000, People's Republic of China*

Complete contact information is available at: https://pubs.acs.org/10.1021/acsomega.3c06290

Notes

The authors declare no competing financial interest.

ACKNOWLEDGMENTS

The financial supports for this work was provided by the Dr. Scientific Research Fund of Yulin University (22GK05), the Youth Innovation Team Research Program Project of Shaanxi Provincial Department of Education (22JP104), the Innovation Capability Support Program of Shaanxi (2020TD-028), the Technology Innovation Leading Program of Shaanxi (2019CGHJ-11), the Science and Technology Plan of Yulin Government (CXY-2020-002-07).

NOMENCLATURE

a	the specific surface area of a solid particle (cm^{-1})
C_f	the concentration of solute in the liquid phase (in terms of the mass of solute per unit volume of solvent) ($g{\cdot}cm^{-3}$)
C_{slR}	the concentration of solute in solid particle at the position $r = R$ ($g{\cdot}cm^{-3}$)
C_s	the average concentration of solute in the solid phase (in terms of the mass of solute per unit volume of the solid matrix) ($g{\cdot}cm^{-3}$)
C^*	the concentration of solute at equilibrium conditions ($g{\cdot}cm^{-3}$)
C_{s0}	initial concentration in the raw material ($g{\cdot}cm^{-3}$)
D_e	effective diffusion coefficient ($m^2{\cdot}s^{-1}$)
k_f	external mass-transfer coefficient film mass-transfer coefficient ($m{\cdot}s^{-1}$)
D_T	the diameter of the vessel (cm)
$D[4,3]$	the volume-averaged particle size of CTR
D_{AB}	the binary diffusion coefficient of solute A (tar) in solvent B (solvent) ($m^2{\cdot}s^{-1}$)
N	impeller speed (min^{-1})
Re_T	Reynolds number based on vessel diameter
Sc	Schmidt number
Sh	Sherwood number based on vessel diameter
R_b	the solvent−solid ratio
R_c	the radius of the stirred vessel (cm)
L	length of the stirred vessel (cm)
ε_p	the porosity of the solid particle
ρ	the density of the liquid ($g{\cdot}cm^{-3}$)
μ	viscosity (mpa·s)
φ	the parameter of association of solvent
$Y_{sim}(t_i)$	yield of tar calculated according to the simulation solution at $t = t_i$, more specifically, it is equal to the simulated extracted tar at $t = t_i$ of the maximum amount of extractable tar (%)
$Y_{exp}(t_i)$	yield of tar from experiment data at $t = t_i$, more specifically, it is equal to the measured extracted tar at $t = t_i$ of the maximum amount of extractable tar (%)

REFERENCES

(1) Ma, Y. H.; Su, W.; Wang, Q. H.; Shao, C. Y.; Huang, X. G.; Yuan, J. Discharge and Disposal of Coking Residue and Distribution Characteristics of PAHs in it. *Appl. Mech. Mater.* **2013**, *448-453*, 448−453.

(2) Wang, X. L.; Shen, J.; Niu, Y. X.; Wang, Y. G.; Sheng, Q. T. Removal of Phenol by powdered activated carbon prepared by residue extracted from coal gasification tar residue. *Environ. Technol.* **2017**, *39* (6), 694−701, DOI: 10.1080/09593330.2017.1310304.

(3) Cheng, J.; Fan, Z.; Si, T.; Zhou, J.; Cen, K. Mechanical strength and combustion properties of biomass pellets prepared with coal tar residue as a binder. *Fuel Process. Technol.* **2018**, *179*, 229−237, DOI: 10.1016/j.fuproc.2018.07.011.

(4) Shen, J.; Wang, X. L.; Niu, Y. X.; Liu, G.; Sheng, Q. T.; Wang, Y. G. Combustion properties and toxicity analysis of coal gasification tar residue. *J. Cleaner Prod.* **2016**, *139* (15), 567−575.

(5) Coulon, F.; Whelan, M. J.; Paton, G. I.; Semple, K. T.; Villa, R.; Pollard, S. J. T. Multimedia fate of petroleum hydrocarbons in the soil: Oil matrix of constructed biopiles. *Chemosphere* **2010**, *81* (11), 1454−1462.

(6) Gao, L.; Dong, F. Q.; Dai, Q. W.; Zhong, G. Q.; Lee, D. J. Coal tar residues based activated carbon: Preparation and characterization. *J. Taiwan Inst. Chem. Eng.* **2016**, *63*, 166−169, DOI: 10.1016/j.jtice.2016.02.029.

(7) Wang, X. L.; Shen, J.; Niu, Y. X.; Sheng, Q. T.; Liu, G.; Wang, Y. G. Solvent extracting coal gasification tar residue and the extracts characterization. *J. Cleaner Prod.* **2016**, *133* (1), 965−970.
(8) Gao, F.; Zhou, C.; Wang, Z.; Zhu, W.; Wang, X.; Liu, G. Solid-oil separation of coal tar residue to reduce polycyclic aromatic hydrocarbons via microwave-assisted extraction. *J. Environ. Manage.* **2023**, *337*, No. 117679, DOI: 10.1016/j.jenvman.2023.117679.
(9) Bomfim, B. P. V.; Moreira, N. M.; Bittencourt, d. A. J.; Elisabete, M. M. Microscale solid-liquid extraction: A green alternative for determination of n-alkanes in sediments. *J. Chromatogr. A* **2022**, *1685*, No. 463635, DOI: 10.1016/j.chroma.2022.463635.
(10) Zhang, L.; Hu, S.; Syed-Hassan, S. S. A.; Xiong, Z.; Xiao, Y.; Jiang, L.; Xu, K.; Wang, Y.; Su, S.; Zhou, Y.; et al. Mechanistic influences of different solvents on microwave-assisted extraction of Shenfu low-rank coal. *Fuel Process. Technol.* **2017**, *166*, 276−281.
(11) Tian, Y.; McGill, W. B.; Whitcombe, T. W.; Li, J. Ionic Liquid-Enhanced Solvent Extraction for Oil Recovery from Oily Sludge. *Energy Fuels* **2019**, *33* (4), 3429−3438.
(12) Wang, Y.; Herdegen, V.; Repke, J.-U. A Model Approach for the Montan Wax Extraction: Model Development and Experimental Analysis. *Sep. Sci. Technol.* **2015**, *50* (15), 2311−2326, DOI: 10.1080/01496395.2015.1056361.
(13) Ho, C. H. L.; Cacace, J. E.; Mazza, G. Mass transfer during pressurized low polarity water extraction of lignans from flaxseed meal. *J. Food Eng.* **2008**, *89* (1), 64−71.
(14) Sánchez, G. M.; Sineiro, T. J.; José, N. M. Extraction of polyphenols from white distilled grape pomace: optimization and modelling. *Bioresour. Technol.* **2008**, *99* (5), 1311−1318, DOI: 10.1016/j.biortech.2007.02.009.
(15) Wang, Y.; Herdegen, V.; Repke, J.-U. Identification and analysis of mass transfer coefficients and effective diffusion coefficients for models of solvent extraction of Montan wax. *Sep. Sci. Technol.* **2016**, *51* (13), 2183−2197, DOI: 10.1080/01496395.2016.1202978.
(16) Wongkittipong, R.; Prat, L.; Damronglerd, S.; Gourdon, C. Solid−liquid extraction of andrographolide from plants—experimental study, kinetic reaction and model. *Sep. Purif. Technol.* **2004**, *40* (2), 147−154.
(17) Simeonov, E.; Koleva, V.; Chilev, C. Solid liquid extraction of furostanal saponins from tribulus terrestris. *J. Univ. Chem. Technol. Metall.* **2011**, *46* (3), 309−314.
(18) Perry, R.; Green, D. *Perry's Chemical Engineers' Handbook*, 7th ed.; McGraw-Hill Education, 2001.
(19) Ghanbarian, B.; Hunt, A. G.; Ewing, R. P.; Sahimi, M. Tortuosity in Porous Media: A Critical Review. *Soil Sci. Soc. Am. J.* **2013**, *77* (5), 1461−1477.
(20) Goto, M.; Smith, J. M.; McCoy, B. J. Kinetics and mass transfer for supercritical fluid extraction of wood. *Ind. Eng. Chem. Res.* **1990**, *29* (2), 282−289.
(21) Ndocko, E. N.; Backer, W.; Strube, J. Process Design Method for Manufacturing of Natural Compounds and Related Molecules. *Sep. Sci. Technol.* **2008**, *43* (3), 642−670, DOI: 10.1080/01496390701812525.
(22) Zizovic, I.; Stamenić, M.; Orlović, A.; Skala, D. Supercritical carbon dioxide essential oil extraction of Lamiaceae family species: Mathematical modelling on the micro-scale and process optimization. *Chem. Eng. Sci.* **2005**, *60* (23), 6747−6756.
(23) Xu, Z.; Shao, H.; Wang, Y.; Zhao, Q.; Liang, Z. Characteristics of coal tar residue treated with microwave-assisted hydrothermal treatment. *Fuel Process. Technol.* **2021**, *211*, No. 106580.
(24) Gaoyun, W.; Le, W.; Linhu, L.; Yunan, C.; Wen, C.; Hui, J.; Zhiwei, G.; Liejin, G. Oil diffusion mathematical model in oily sludge particle under supercritical water environment. *J. Hazard. Mater.* **2022**, *443* (Pt B), No. 130348, DOI: 10.1016/j.jhazmat.2022.130348.
(25) Xian, F.; Dong, L.; Junghui, C.; Menglong, N.; Xu, L.; Teck, C. L. L.; Wenhong, L. Kinetic parameter estimation and simulation of trickle-bed reactor for hydrodesulfurization of whole fraction low-temperature coal tar. *Fuel* **2017**, *230*, 113−125, DOI: 10.1016/j.fuel.2018.05.023.
(26) Cussler, E. L. Diffusion: Mass Transfer in Fluid Systems. *Q. Rev. Biol.* **1987**, *62*, 146−177, DOI: 10.1086/415398.
(27) Prommuak, C.; Tharangkool, N.; Pauasant, P.; Ponpesh, P.; Jarunglumlert, T. Computational fluid dynamic design of spent coffee ground cabinet dryer using recycled heat from air compressor. *Chem. Eng. Res. Des.* **2020**, *153*, 75−84, DOI: 10.1016/j.cherd.2019.10.017.
(28) Wang, Y.; Herdegen, V.; Li, X.; Repke, J.-U. Numerical study and evaluation of solid-liquid extraction of Montan wax in stirred tanks on different scales. *Sep. Purif. Technol.* **2018**, *204*, 90−97.
(29) Cao, Y.; Wang, X.; Xie, J.-H. The infinite Schmidt number limit of the salt fingering convection model and the inertial free salt convection model. *Mech. Res. Commun.* **2023**, *127*, No. 104024.
(30) Humphrey, D. W.; Ness, H. C. V. Mass transfer in a continuous-flow mixing vessel. *AIChE J.* **1957**, *3* (2), 283−286, DOI: 10.1002/aic.690030227.
(31) Wakao, N.; Smith, J. M. Diffusion in catalyst pellets. *Chem. Eng. Sci.* **1962**, *17* (11), 825−834.
(32) Chang, H.-C. Multi-scale analysis of effective transport in periodic heterogeneous media. *Chem. Eng. Commun.* **1982**, *15* (1−4), 83−91.
(33) Burstein, L.ODE-, PDEPE-Solvers, and PDE Modeler tool with Applications. In *A MATLAB Primer for Technical Programming in Materials Science and Engineering*; Elsevier, 2020; pp 205−258.
(34) Nie, J.; Chen, D.; Ye, J.; Lu, Y.; Dai, Z. Optimization and Kinetic Modeling of Ultrasonic-Assisted Extraction of Fucoxanthin from Edible Brown Algae Sargassum fusiforme Using Green Solvents. *Ultrason. Sonochem.* **2021**, *77*, No. 105671.
(35) Pasquet, V.; Chérouvrier, J.-R.; Farhat, F.; Thiéry, V.; Piot, J.-M.; Bérard, J.-B.; Kaas, R.; Serive, B.; Patrice, T.; Cadoret, J.-P.; et al. Study on the microalgal pigments extraction process: Performance of microwave assisted extraction. *Process Biochem.* **2011**, *46* (1), 59−67.
(36) Qu, W.; Pan, Z.; Ma, H. Extraction modeling and activities of antioxidants from pomegranate marc. *J. Food Eng.* **2010**, *99* (1), 16−23.
(37) Amarante, R. C. A.; Oliveira, P. M.; Schwantes, F. K. Oil Extraction from Castor Cake Using Ethanol: Kinetics and Thermodynamics. *Ind. Eng. Chem. Res.* **2014**, *53* (16), 6824−6829, DOI: 10.1021/ie500508n.
(38) Kitanović, S.; Milenović, D.; Veljković, V. B. Empirical kinetic models for the resinoid extraction from aerial parts of St. John's wort (*Hypericum perforatum* L.). *Biochem. Eng. J.* **2008**, *41* (1), 1−11.
(39) Menkiti, M. C.; Agu, C. M.; Udeigwe, T. K. Extraction of oil from Terminalia catappa L.: Process parameter impacts, kinetics, and thermodynamics. *Ind. Crops Prod.* **2015**, *77*, 713−723.
(40) Sonja, J.; Milan, M.; Biljana, A.; Vesna, S. J. The kinetic and thermodynamic studies of solid-liquid extraction of apigenin-glycosides from parsley (*Petroselinum crispum*). *Sep. Sci. Technol.* **2021**, *56* (13), 2253−2265, DOI: 10.1080/01496395.2020.1821219.
(41) Döker, O.; Salgın, U.; Şanal, İ.; Mehmetoğlu, Ü.; Çalımlı, A. Modeling of extraction of β-carotene from apricot bagasse using supercritical CO2 in packed bed extractor. *J. Supercrit. Fluids* **2004**, *28* (1), 11−19.
(42) Hu, G.; Li, J.; Hou, H. A combination of solvent extraction and freeze thaw for oil recovery from petroleum refinery wastewater treatment pond sludge. *J. Hazard. Mater.* **2015**, *283*, 832−840.
(43) Si, T.; Cheng, J.; Zhou, F.; Zhou, J.; Cen, K. Control of pollutants in the combustion of biomass pellets prepared with coal tar residue as a binder. *Fuel* **2017**, *208* (15), 439−446.
(44) Zhang, J.; Li, J.; Thring, R. W.; Hu, X.; Song, X. Oil recovery from refinery oily sludge via ultrasound and freeze/thaw. *J. Hazard. Mater.* **2011**, *203* (15), 195−203, DOI: 10.1016/j.jhazmat.2011.12.016.

https://doi.org/10.1021/acsomega.3c06290
ACS Omega 2023, 8, 47835−47845